Eco-Engineered Functionalized Mesoporous Silica from Rice Husk for Selective Detection of Fe(III) in Aqueous Media

A. Subaihi[1], B.A. Babgi[2], T.S. Alraddadi[3], T.Z. Abolibda[3], M.T. Alotaibi[4], A.K. Albishri[5], A. Shahat[3,*], M.A. Shenashen[6,*]

[1]Department of Chemistry, University College in Al-Qunfudhah, Umm Al-Qura University, Saudi Arabia

[2] Department of Chemistry, Faculty of Science, King Abdulaziz University (KAU), Jeddah 21589, Saudi Arabia

[3] Chemistry Department, Faculty of Science, Islamic University of Madinah, Madinah, 42351, Saudi Arabia

[4]Department of Chemistry, Turabah University College, Taif University, P.O. Box 11099, Taif 21944, Saudi Arabia

[5]Department of Chemistry, College of Sciences & Arts, King Abdulaziz University, Rabigh, Kingdom of Saudi Arabia

[6] Department of Petrochemical, Egyptian Petroleum Research Institute (EPRI), Nasr City, 11727, Cairo, Egypt

*Corresponding authors: mashenashen@gmail.com (Prof. M.A. Shenashen); ashahat@aucegypt.edu (Prof. A. Shahat)

1.1. Materials and Reagents

All reagents were of analytical grade and used without further purification unless otherwise stated. 1,6-Dihydroxy-2-naphthaldehyde (CAS: 4900-62-9, 98% purity), 4-bromoaniline (CAS: 106-40-1, 98% purity), and 2-aminophenol (CAS: 95-55-6, 99% purity) were procured from Sigma-Aldrich (St. Louis, USA) and used as received for the synthesis of BMN and HMN Schiff base probes.

Ferric chloride hexahydrate ($FeCl_3 \cdot 6H_2O$, CAS: 10025-77-1, ≥99% purity) and ethylenediaminetetraacetic acid (EDTA, CAS: 60-00-4, 99.4% purity) were obtained from Merck (Darmstadt, Germany). Sodium hydroxide (NaOH, CAS: 1310-73-2, 98% purity) and sulfuric acid (H_2SO_4, CAS: 7664-93-9, 95-98% purity) were of reagent grade from Merck (Germany).

Hydrochloric acid (HCl, CAS: 7647-01-0, 37% w/w, density 1.19 g/mL), absolute ethanol (CAS: 64-17-5, 99.9% purity), and all buffer components [2-chloroacetic acid ($ClCH_2COOH$, 99%), acetic acid (CH_3COOH, 99.8%), CHES (N-cyclohexyl-2-aminoethanesulfonic acid, 99.5%), and MOPS (3-(N-morpholino)propanesulfonic acid, 99%)] were of analytical/reagent grade and purchased from Alfa Aesar (Heysham, UK).

Deionized water (resistivity >18.2 MΩ·cm, Type 1 ultrapure water, Millipore system) was used throughout all experiments. All chemicals were used without additional purification unless explicitly stated.

1.2. Synthesis of Schiff Base Probes

1.2.1. Synthesis of (E)-2-(((4-bromophenyl)imino)methyl)naphthalene-1,6-diol (BMN)

BMN's Schiff base was synthesized by a condensation reaction between 1,6-dihydroxy-2-naphthaldehyde and 4-bromoaniline (**Scheme 1B**). To ensure everything dissolved properly, 1.88 g (10 mmol) of 1,6-dihydroxy-2-naphthaldehyde was mixed with 30 mL of ethanol while being

gently heated and stirred with a magnetic stirrer. To improve reaction kinetics control and minimize side reactions, 1.72 g (10 mmol) of 4-bromoaniline was mixed in 10 mL of ethanol and then introduced dropwise to the aldehyde solution over a period of 15 minutes in a different vessel. After that, the reaction mixture was refluxed for 4 hours at 65°C while being constantly stirred. A yellow Schiff base product started to form throughout this period. The solid was separated by vacuum filtration after it had cooled to room temperature, repeatedly cleaned with cold ethanol to get rid of any remaining reactants or contaminants, and then vacuum-dried for 12 hours at 60°C. With an 89% yield, or 3.2 g, the end product, BMN, was produced as vibrant yellow crystals.

BMN: Yield: 84%. **^{1}H NMR (d_6-DMSO, 300 MHz) δ:** 14.32 (s, 1H, OH), 9.22 (s, 1H, OH), 8.94 (s, 1H, CH=N), 8.05 (d, *J* = 7.5 Hz, 1H, Ar-H), 7.76–7.38 (m, 7H, Ar-H), 7.03 (d, *J* = 7.8 Hz, 1H, Ar-H. **^{13}C NMR (d6-DMSO, 125 MHz) δ:** 168.6 (C=O), 161.6 (C=N), 153.8, 152.8, 141.2, 135.5, 133.4, 131.5, 130.7, 128.6, 122.6, 121.0, 116.2, 115.5, 108.2. **CHNO analysis**: %C 59.67 (59.55), %H 3.53 (3.49), %Br 23.35 (23.15), %N 4.09 (4.01), %O 9.35 (9.21); theoretical data in parentheses.

1.2.2. Synthesis of (E)-2-(((2-hydroxyphenyl)imino)methyl)naphthalene-1,6-diol (HMN)

A condensation reaction that is comparable to that of BMN was used to synthesize HMN. Using this procedure, 30 mL of ethanol was gradually stirred to dissolve 1.88 g (10 mmol) of 1,6-dihydroxy-2-naphthaldehyde (Scheme 1B). To avoid oxidizing the hydroxyl groups, 1.09 g (10 mmol) of 2-aminophenol was added gradually to the aldehyde solution while being dissolved in 10 mL of ethanol. After 4 hours of refluxing the resultant mixture at 65°C, an orange solid that was a sign of HMN production started to slowly form. Following room temperature cooling, the solid product was separated by vacuum filtration, rinsed well with cold ethanol to eliminate any

remaining reactants, then vacuum-dried for 12 hours at 50°C to maintain the product's integrity. 2.5 grams of the final HMN compound were obtained as an orange crystalline powder.

HMN: Yield: 84%. **^{1}H NMR (d_6-DMSO, 300 MHz)** δ: 15.43 (s, 1H, OH), 9.85 (s, 1H, OH), 9.22 (s, 1H, OH), 8.67 (s, 1H, CH=N), 8.05 (d, *J* = 7.5 Hz, 1H, Ar-H), 7.67 (d, *J* = 7.5 Hz, 1H, Ar-H), 7.45 (m, 1H, Ar-H), 7.17 (t, *J* = 7.5 Hz, 1H, Ar-H), 7.05 (d, *J* = 7.5 Hz, 1H, Ar-H), 6.97 (d, *J* = 7.5 Hz, 1H, Ar-H), 6.92 (t, *J* = 7.5 Hz, 1H, Ar-H), 6.87 (d, *J* = 7.5 Hz, 1H, Ar-H), 6.81 (d, *J* = 7.5 Hz, 1H, Ar-H). **^{13}C NMR (d6-DMSO, 125 MHz)** δ: 168.6, 153.8, 152.8, 151.5, 141.2, 133.4, 131.5, 130.7, 128.3, 122.6, 121.0, 120.2, 119.8, 116.2, 115.5, 108.2. **CHNO analysis**: %C 73.02 (73.11), %H 4.61 (4.69), %N 5.06 (5.02), and %O 17.11 (17.19); the theoretical data have been implicated in parentheses.

1.3. Production protocol of rice husk (RH)-derived mesoporous silica platform (MSP)

Initially, collected raw RH were carefully rinsed with deionized water to remove dust, dirt, and water-soluble contaminants, followed by drying at 105°C for 24 hours in a laboratory oven. Mineral impurities, particularly potassium, calcium, and iron, that could otherwise form stable silicates after calcination were successfully removed from the dried RHs by subjecting them to acid treatment using 1 M hydrochloric acid at 80°C for 2 hours with constant stirring.

Following acid leaching, the treated RHs were rinsed with DI water until reaching neutral pH and then dried again overnight at 105°C. To remove organic components and produce an amorphous bio-silica structure, the dried RH was calcined at 650°C for 4 hours (with a ramp rate of 10°C/min) [45]. In order to enhance surface area for the subsequent procedures, the resultant white rice husk ash (RHA) was ground into a fine powder. A soluble sodium silicate solution was produced by treating this RHA powder with 2 M sodium hydroxide (10 g RHA in 100 mL solution) for 2 hours at 90°C. The solution was then vacuum filtered to remove residual solids.

The transparent sodium silicate solution was progressively acidified with 2 M sulfuric acid while being constantly stirred until the pH reached 7.0 in order to precipitate pure silica. To enhance its structural and textural qualities, the resultant silica gel was aged for 24 hours at room temperature. The gel was dried for 24 hours at 105°C after being aged and rinsed with deionized water to remove sodium sulfate and other residues. In order to produce high-purity silica nanoparticles with advantageous surface qualities for additional uses, the dry gel was lastly crushed into a fine powder and calcined for three hours at 500°C.

2.1. FTIR Spectroscopy analysis for BMN@MSP and HMN@MSP materials

The FTIR spectra of BMN@MSP and HMN@MSP provide definitive spectroscopic evidence for successful immobilization of both Schiff-base ligands onto the mesoporous silica framework and reveal critical differences in their surface chemistry and hydrogen bonding interactions that directly correlate with their distinct Fe(III) sensing performance. Upon immobilization of BMN and HMN, both composite materials retain the intense Si–O–Si stretching bands, confirming that the silica backbone structure remains fundamentally intact after functionalization. Superimposed on the silica framework bands, new absorption features uniquely attributable to the organic Schiff-base ligands emerge: both BMN@MSP and HMN@MSP show a strong, sharp imine C=N stretching band in the 1610–1630 cm^{-1} region, which is completely absent in unmodified MSP. This band is diagnostic for the azomethine (C=N) functionality and constitutes unequivocal proof that the Schiff-base ligands have been successfully retained on the silica surface through the immobilization process. The preservation of the characteristic imine stretch confirms that the critical metal-coordinating imine nitrogen remains intact and available for Fe(III) complexation.

In the aromatic region (1500–1600 cm^{-1}), both sensors display distinct C=C stretching vibrations characteristic of the naphthalene backbone system, confirming that the π-conjugated aromatic

cores of both ligands are preserved on the surface. Both BMN@MSP and HMN@MSP show dramatically broadened O–H stretching absorption that extends across the entire 3200–3600 cm^{-1} window, with notably greater breadth and intensity in the HMN@MSP spectrum compared to BMN@MSP. This broadening is a classic signature of hydrogen bonding, where the local environment of O–H groups becomes heterogeneous due to interactions with adjacent electron-rich sites (oxygen atoms of phenolic OH groups and nitrogen atoms of imine groups). The enhanced breadth of the O–H absorption in HMN@MSP directly reflects HMN's possession of three phenolic hydroxyl groups compared to BMN's single hydroxyl group, resulting in more extensive hydrogen bonding networks between the ligand and the silica surface (Si–OH···O hydrogen bonds) and among the ligand's hydroxyl groups themselves (O–H···N intramolecular interactions). Quantitatively, the O–H stretch in HMN@MSP spans from ~3200 cm^{-1} (most strongly hydrogen-bonded species) to ~3600 cm^{-1} (weakly hydrogen-bonded or free silanols), indicating a distribution of bonding environments. This extensive hydrogen bonding capability is mechanistically significant: it creates a "hard-soft acid-base" coordination sphere on the HMN@MSP surface where the hydroxyl oxygen atoms and imine nitrogen atom work in concert to stabilize hard metals like Fe(III), explaining HMN@MSP's superior binding affinity and selectivity compared to BMN@MSP.

In the C–O stretching region (1200–1300 cm^{-1}), the intensity of this band at ~1270 cm^{-1} is notably enhanced in HMN@MSP relative to BMN@MSP, directly corresponding to HMN's three phenolic OH groups versus BMN's single OH group. The presence and prominence of phenolic C–O stretches confirm that the electron-donating phenolic oxygen atoms are successfully immobilized and available for metal coordination. At ~1620 cm^{-1}, overlapping with the C=N imine stretch, aromatic C=C vibrations contribute a strong absorption band, with greater intensity in

HMN@MSP, again consistent with the higher ligand loading (and correspondingly higher aromatic content) in HMN@MSP.

A subtle but important feature appears in the 2800–3000 cm^{-1} region, where C–H stretching vibrations from the aromatic and aliphatic portions of the ligands give rise to weak but distinct absorptions. These bands are visible in both sensors and confirm the presence of organic matter, with slightly greater prominence in HMN@MSP reflecting its higher organic content. The fingerprint region (500–1000 cm^{-1}) shows complex multiplet patterns arising from Si–O stretching and Si–O–Si bending modes, and these patterns are essentially unchanged between BMN@MSP and HMN@MSP, indicating that the fundamental silica framework topology is preserved.

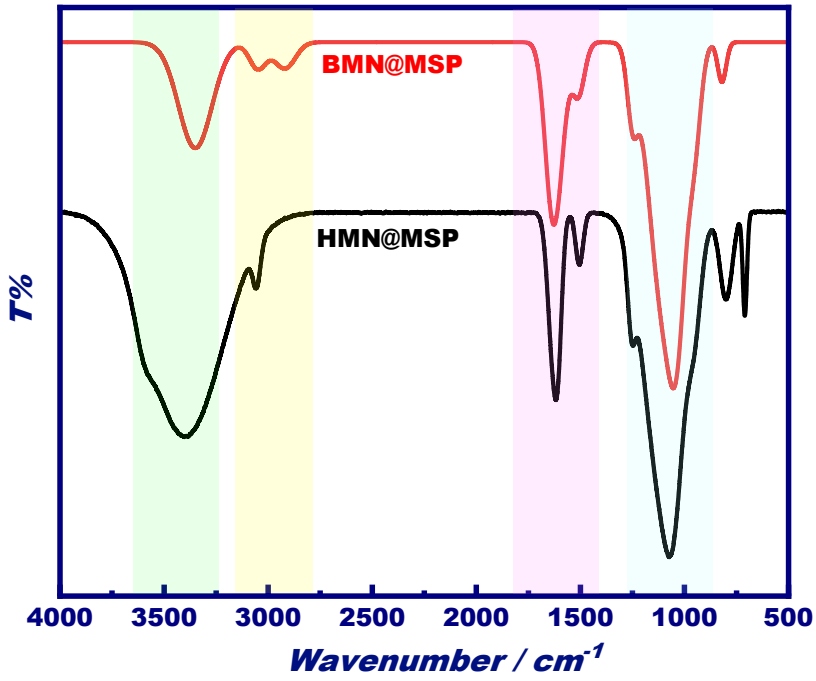

SI: Figure 1. FTIR analysis for the BMN@MSP and HMN@MSP materials

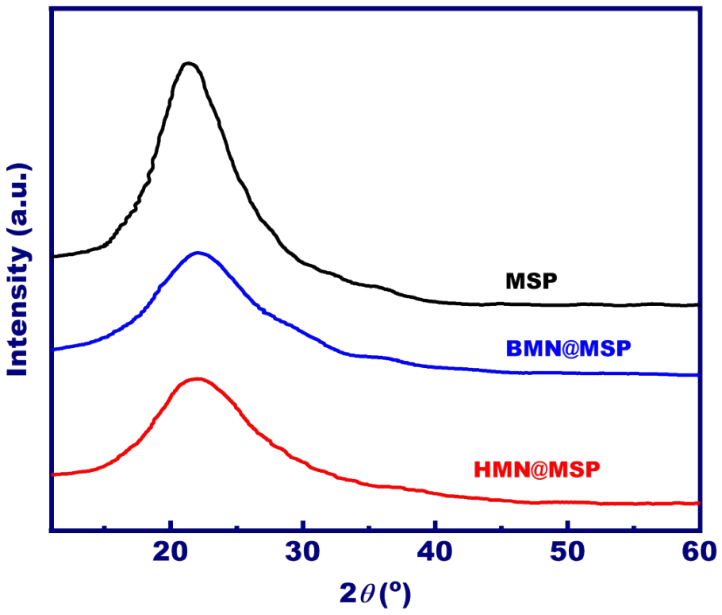

SI: Figure 2. XRD analysis for MSP, HMN@MSP, and BMN@MSP materials

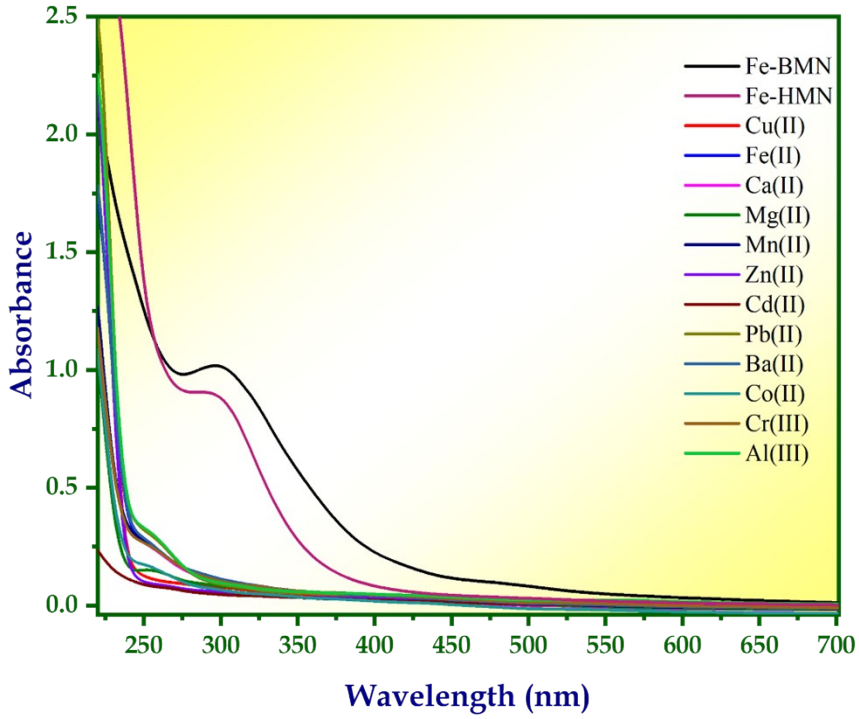

SI: Figure 3. Absorption spectrum for the selectivity of Fe(III) with the BMN and HMN in the presence of other competing ions.

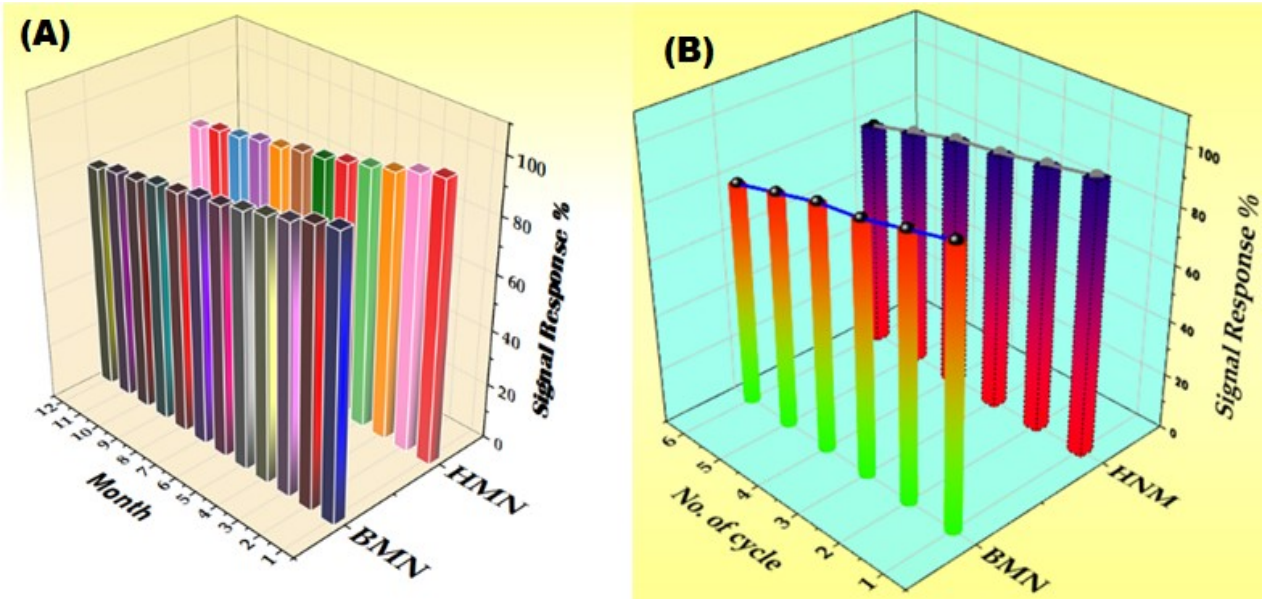

SI: Figure 4: Stability and regeneration performance of the BMN@MSP and HMN@MSP: (A) Long-term stability of the synthesized platforms; (B) Reusability studies.

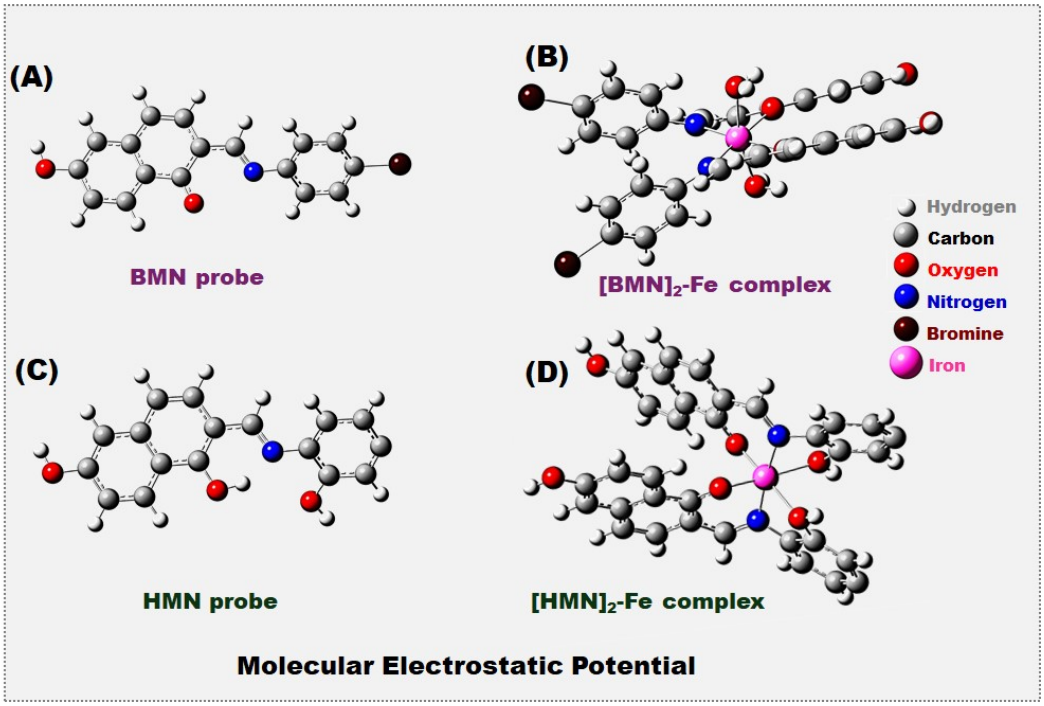

SI: Figure 5: Optimized geometry structures for (A) BMN probe, (B) $[BMN]_2$-Fe complex, (C) HMN probe, and (D) $[HMN]_2$-Fe complex.

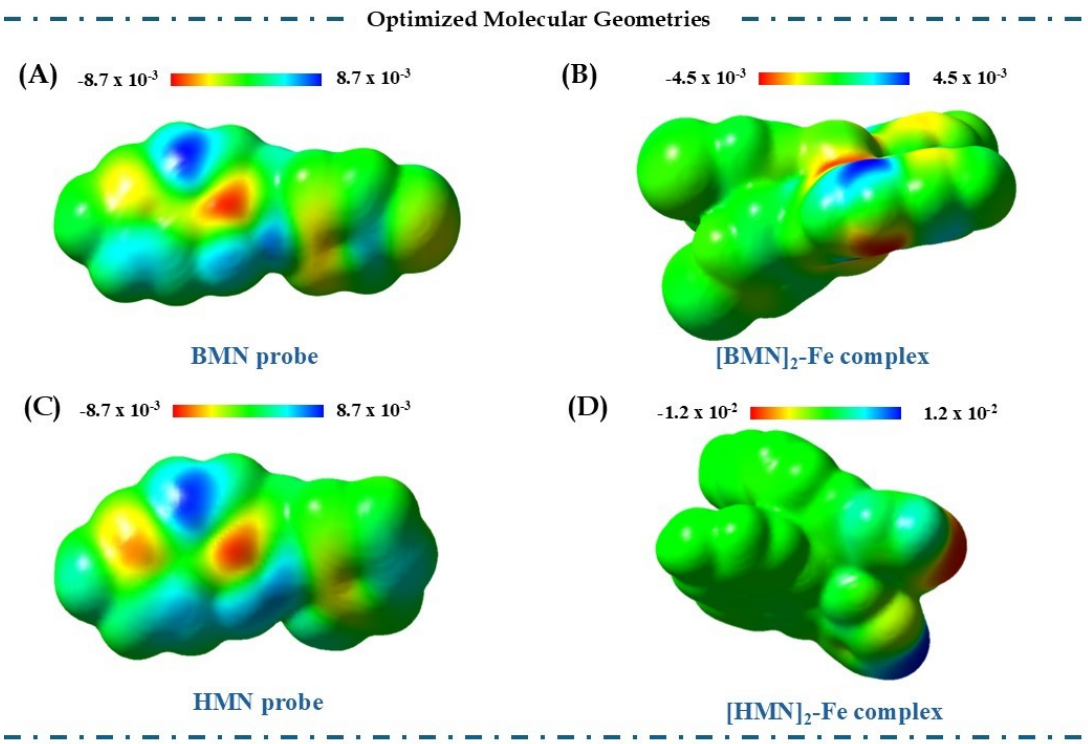

SI: Figure 6: Molecular electrostatic potential (MEP) for (A) BMN probe, (B) $[BMN]_2$-Fe complex, (C) HMN probe, and (D) $[HMN]_2$-Fe complex.

SI: Figure 7. Molecular Orbitals (FMOs) of the (A) BMN probe, (B) $[BMN]_2$-Fe complex, (C) HMN probe, and (D) $[HMN]_2$-Fe complex, where regions of positive potential are depicted in light blue and negative potential are shown in orange.

	LUMO	HOMO	-ΔE
BMN probe	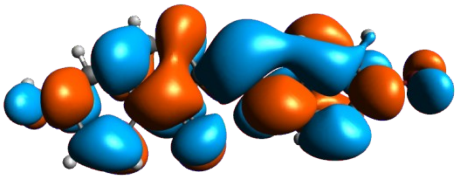 **-1.965 eV**	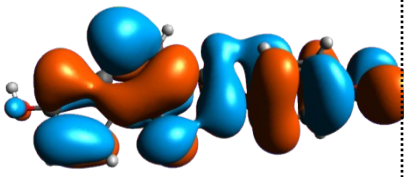 **-5.865 eV**	**3.9 eV**
$[BMN]_2$-Fe complex	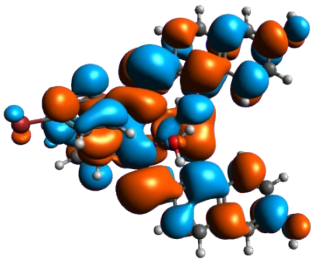 **-1.976 eV**	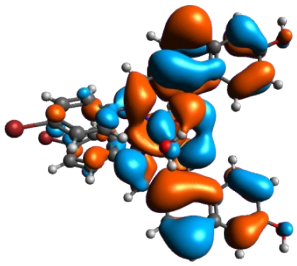 **-5.631 eV**	**3.655 eV**
HMN probe	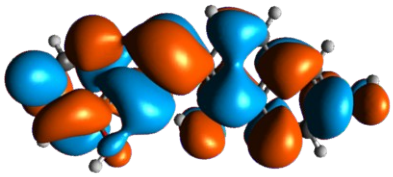 **-1.924 eV**	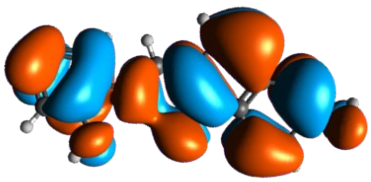 **-4.974 eV**	**3.05 eV**
$[HMN]_2$-Fe complex	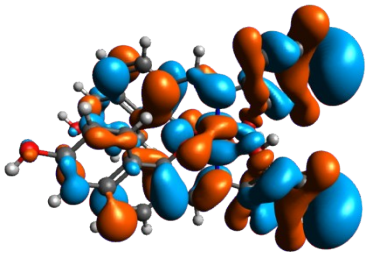 **-4.320 eV**	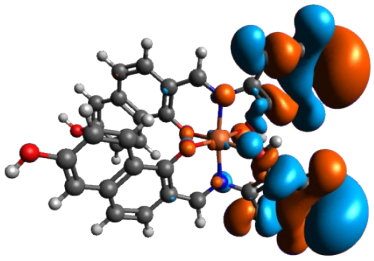 **-4.815 eV**	**0.495 eV**